

# Anomaly of the geomagnetic Sq variation in Japan: effect from 3-D subterranean structure or the ocean effect?

Alexei Kuvshinov<sup>1,2</sup> and Hisashi Utada<sup>2</sup>

<sup>1</sup>*Institute of Geophysics, ETH, Sonneggstrasse 5, CH-8092 Zurich, Switzerland. E-mail: kuvshinov@erdw.ethz.ch*

<sup>2</sup>*Ocean Hemisphere Research Center, Earthquake Research Institute, University of Tokyo, Yayoi 1-1-1, Bunkyo-ku, Tokyo 113-0032, Japan*

Accepted 2010 September 11. Received 2010 May 13; in original form 2009 September 21

## SUMMARY

Many years ago Rikitake *et al.* described the anomalous behaviour of the vertical component  $Z$  of the geomagnetic solar quiet (Sq) daily variation field at observatories in central and northern Japan – namely about 2 hr shift of the local noontime peak towards morning hours. They suggested that this anomaly is associated with the anomalous distribution of electrical conductivity in the mantle beneath central Japan. Although a few works have been done to confirm or argue this explanation, no clear answer has been obtained so far. The goal of this work is to understand the nature of this anomaly using our 3-D forward solution. The conductivity model of the Earth includes oceans of laterally variable conductance and conducting mantle either spherically symmetric or 3-D underneath. Data from six Japanese observatories at four seasons for two different years of the solar cycle are analysed. As an inducing ionospheric (Sq) current system, we use those provided by the Comprehensive Model (CM4) of Sabaka *et al.* Our analysis clearly demonstrates that 3-D induction in the ocean is responsible for the anomalous behaviour of  $Z$  daily variations in this region. We also show that the effects from a suite of 3-D mantle models that include mantle wedge and subducting slab are minor compared with the ocean effect.

**Key words:** Numerical solutions; Geomagnetic induction; Magnetic field.

## 1 INTRODUCTION

Geomagnetic solar quiet (Sq) daily variations observed at ground primarily originate from the current system flowing in the ionospheric  $E$ -layer at an altitude of about 110 km. This current system is driven by solar tidal winds and spread within a latitudinal limit of  $\pm 60^\circ$  on the sunlit side of the Earth, with an anticlockwise (clockwise) whorl in the Northern (Southern) Hemisphere. Viewed from the Sun, the Earth rotates underneath this ionospheric current system and therefore Sq variations are mainly local time (LT) phenomena. More information on geomagnetic Sq variations in general is available from Campbell (1989). Besides the primary effect of Sq ionospheric currents, observations of geomagnetic variations contain a part coming from secondary currents induced in the solid Earth and the oceans by the time-varying magnetic field of ionospheric origin. From the geometry of the Sq current system and from an assumption that the electrical conductivity of the Earth is 1-D, that is, conductivity depends only on depth, one can expect a peak (negative/positive in Northern/Southern Hemisphere) of the vertical component  $Z$  of the geomagnetic Sq daily variation around 12:00 LT.

More than 50 years ago Rikitake *et al.* (1956) described anomalous behaviour of the vertical component  $Z$  of the geomagnetic Sq daily variation field at observatories in central and northern Japan – namely about a two-hour shift of the local noontime peak towards

morning hours. They also noted that this effect is absent at a site located in the southwestern part of Japan. It was suggested that this anomaly in  $Z$  may not be explained by the electromagnetic (EM) induction in the conducting sea when the large field penetration depth is considered but should be associated with low electrical conductivity in the mantle beneath central Japan.

For decades this problem remained unresolved mostly due to the lack of numerical tools for accurate and detailed calculations of Sq variations in substantially 3-D environment of the region of interest. However, during the last decade or so significant methodological progress has been made to tackle various global induction problems with adequate levels of complexity and spatial detail in both 3-D electrical conductivity models and the sources. Takeda (1993) studied the phenomenon by using thin-sheet modelling and also concluded that the anomaly in  $Z$  variations could not be explained only by the ocean induction effect. However, this conclusion was rather weak because the external (inducing) and internal (induced) fields were not properly separated in that paper. Later Kuvshinov *et al.* (1999) and Kuvshinov *et al.* (2007), based on 3-D model studies with a realistic Sq source, indicated that the anomaly of Sq variations in Japan is most likely generated by induction in the ocean.

The main aim of this paper is to confirm, on the representative data, the oceanic nature of this anomaly. This work is also based on

3-D model studies and exploits a conductivity model of the Earth, which includes oceans and continents of laterally variable near-surface conductance and a conducting mantle either spherically symmetric or 3-D underneath. Data from six Japanese observatories at four quiet days from four seasons and from two different years of the solar cycle are analysed. As for the model of the inducing ionospheric Sq current system, we use those provided by the Comprehensive Model (CM4) of Sabaka *et al.* (2004). Comparison of observations and predictions clearly demonstrates that the induction in the ocean is a major player in forming such anomalous behaviour of  $Z$  daily variations in this region. To support this point further, we compare predictions and observations at an inland observatory in China. The behaviour of  $Z$  at this station is shown to be explained simply by the 1-D model. We also examine how the changes in the near-surface conductance map affect the computed  $Z$  variations. Finally, we estimate effects from 3-D structures such as the subducting slab (with and without enhanced conductivity in the transition zone) and the mantle wedge and examine whether these effects are comparable with the effect from the ocean.

## 2 FORWARD COMPUTATION OF MAGNETIC FIELDS INDUCED BY Sq SOURCE

Global EM induction computations require a model of the electrical conductivity of the Earth's interior. Our basic (3-D) model consists of a thin spherical shell of variable conductance at the Earth's surface over a spherically symmetric (1-D) mantle. The shell conductance is obtained by considering contributions both from sea water and from sediments. The conductance of the sea water has been taken from Manoj *et al.* (2006) and accounts for ocean bathymetry (taken from the global  $5' \times 5'$  NOAA ETOPO map of bathymetry/topography), ocean salinity, temperature and pressure as given by the World Ocean Atlas 2001 ([www.ngdc.noaa.gov](http://www.ngdc.noaa.gov)). Conductance of the sediments (in continental as well as oceanic regions) is based on the global sediment thicknesses given by the  $1^\circ \times 1^\circ$  map of Laske & Masters (1997) and calculated by a heuristic procedure similar to that described in Everett *et al.* (2003). The resolution of the model is  $1^\circ \times 1^\circ$  in colatitude and longitude. The 1-D conductivity model is taken from Shimizu *et al.* (2010), where the authors constructed a 1-D model for the North Pacific Ocean – just for the region of our interest.

Daily variations of the magnetic field due to Sq source within 1-D and 3-D conductivity models of the Earth are calculated as follows.

(1) We derive the time harmonics of the inducing current system for a particular day by taking Fourier transform of the time series consisting of hour-by-hour snapshots of the ionosphere current systems provided by CM4. We consider only the first six time harmonics ( $p = 1 - 6$ ) with periods  $24/p$  between 24 and 4 hr; harmonics higher than  $p = 6$  have relatively small amplitude and are not considered in our analysis (cf. Schmucker 1999).

(2) For each time harmonic, we perform EM induction simulations using 1-D (i.e. without oceans) and 3-D (with oceans) models of electrical conductivity. To simulate magnetic fields, the frequency-domain integral equation solution (cf. Kuvshinov 2008) is used.

(3) The time-series of resulting daily variations are obtained by means of an inverse Fourier transform of the frequency-domain results.

## 3 COMPARISON OF OBSERVATIONS WITH PREDICTIONS

### 3.1 Effect from Sq source variability

We now compare the simulated daily variations with observatory data. For analysis we have chosen two years with different levels of solar activity, namely 1997 (quieter) and 2000 (more disturbed). Data from seven observatories are analysed. Six of them are located in Japan and one in China. The Japanese observatories are Memambetsu (MMB;  $\vartheta = 46.09^\circ$ ,  $\varphi = 144.19^\circ$ ), Mizusawa (MIZ;  $\vartheta = 50.89^\circ$ ,  $\varphi = 141.20^\circ$ ), Kakioka (KAK;  $\vartheta = 53.77^\circ$ ,  $\varphi = 140.19^\circ$ ), Kanozan (KNZ;  $\vartheta = 54.74^\circ$ ,  $\varphi = 139.96^\circ$ ), Hatizyo (HTY;  $\vartheta = 56.93^\circ$ ,  $\varphi = 139.83^\circ$ ), Kanoya (KNY;  $\vartheta = 58.58^\circ$ ,  $\varphi = 130.88^\circ$ ) and the Chinese observatory is Beijing Ming Tombs (BMT;  $\vartheta = 49.70^\circ$ ,  $\varphi = 116.2^\circ$ ). Fig. 1 shows their location along with the conductance map in this region. It is seen that all Japanese observatories are located in the coastal zones where large lateral contrasts of conductance exist. This is especially true for five observatories (MMB, MIZ, KAK, KNZ and HTY) situated in central and northern parts of Japan. KNY is also located near the coast but with the conductance contrast slightly weaker than for other five observatories. The Chinese observatory BMT is located far inland from the deep ocean and thus from the large lateral contrasts of conductance. As expected data from this site does not reveal anomalous behaviour (we will see this later) and is used in our model studies for normalizing predictions at the Japanese observatories.

To make our analysis as conclusive and as consistent with the discussion in Rikitake *et al.* (1956) as possible we consider the data from four (winter, spring, summer and autumn) seasons. Since we are interested to see 3-D induction effects in its clearest form we adhere to analysis of daily variations under magnetic quiet conditions. Another influential decision is to use single days for analysis, instead of averaging over the quietest days of each season. This decision is mostly governed by the fact that as inducing ionospheric (Sq) current systems we use those provided by the CM4. As it is stated in the CM4 description this model allows for calculating the ionospheric current system for any day, provided the user multiplies the predictions by a value of  $F_{10.7}$  for this day. However, our previous experience with CM4 (cf. Kuvshinov *et al.* 2007) is that often one has to multiply predictions for the selected day with a factor which differs from  $F_{10.7}$ . This in particular means that averaging the predictions to make them compatible with the averaged observations leaves rather large room for subjectivity, which we intend to avoid.

The selection of suitable days follows the quietness definition introduced by Schmucker (1999). We understand that this definition involves several problems (Everett 2006) which however are not very serious in the present case of answering Rikitake's question. It is based on a fixed upper limit for a specified sum of 3-hr  $ap$  indices. This sum contains not only the eight indices of the considered day, but also the eight indices of the 12 hr before and after. If the sum of all 16  $ap$  indices does not exceed 60, the day is declared as quiet and termed a  $Q^*$ -day. Specifically for each season we work with a single  $Q^*$ -day, thus analysing in overall eight  $Q^*$ -days. The selected days for the quieter year (1997) are: January 5 (100/74.4), March 19 (100/73.7), June 14 (110/73.5) and October 5 (180/84.4). The first and second numbers in brackets are the multiplication factor we use and the observed value of  $F_{10.7}$  for this day, respectively. Note that the multiplication factor for each day is chosen by minimizing the difference between predicted (in the model with oceans) and observed variations at the 'normal' Chinese observatory BMT.

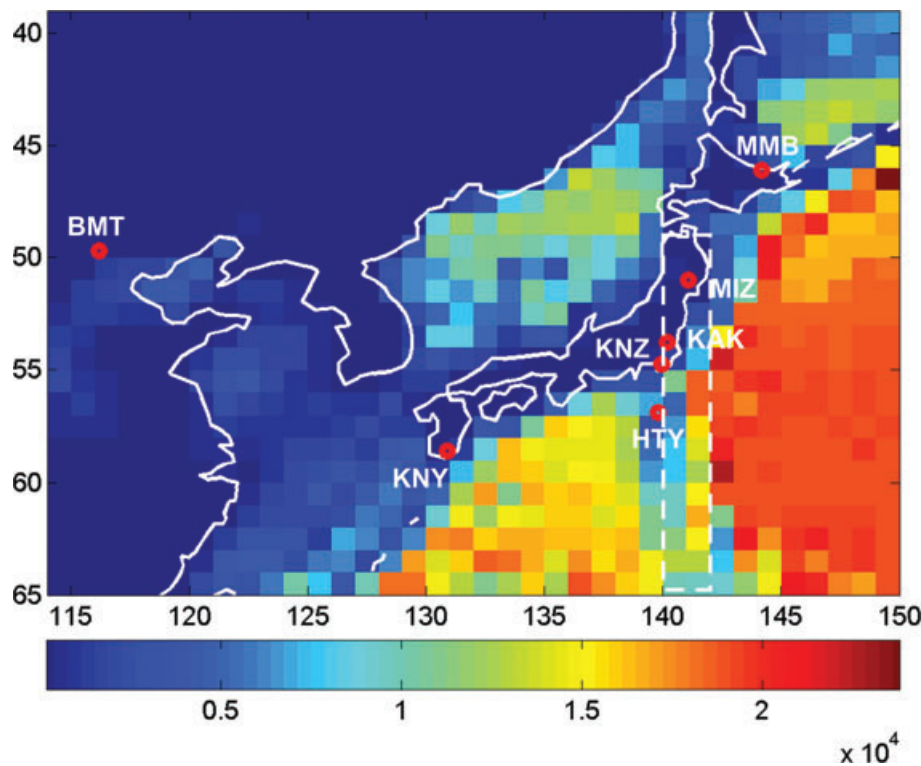


**Figure 1.** Conductance (in S) map in the region and location of observatories. Dashed white line depicts the projection of the slab's roof onto the Earth's surface. See the side view of the model with the slab in Fig. 7.

The selected days for the more disturbed year (2000) are: January 18 (210/194.6), March 17 (200/192.4), August 18 (230/169.5) and October 21 (160/158.0). The choice of a different summer month (August) for 2000 instead of June in 1997 is explained by the fact that there are no Q\*-days in June and July of 2000. Figs 2 and 3 present the predicted and observed daily variations of  $Z$  as a function of LT for six Japanese observatories on four selected days, for 1997 and 2000, respectively. Observations, 1-D (without oceans) and 3-D (with oceans) predictions are depicted by black (with circles), blue and red lines, respectively. Note that we subtracted from the hourly mean observations an estimate of the 'true' baseline (rather than the value around midnight), which we calculate as the difference between the observed daily mean and that of the external field contribution, as was argued for in appendix A of Schmucker (1999).

By inspecting plots in these two figures we observe that predictions in the 3-D model with the ocean (red lines) do reproduce the shift of the local noontime peak towards morning hours at five observatories located in central and northern Japan. It is interesting that 3-D predictions don't show such a shift at the KNY observatory located in the southwestern part of Japan; this is also in fair agreement with what Rikitake *et al.* (1956) observed at the Aso observatory located about 100 km to the north of KNY.

It is seen from the figures that the agreement is overall better for the more disturbed year (2000); the concordance is especially good, both regarding peak-to-peak magnitude and the shape of the signals, for the winter day of 2000 and for the spring day to a slightly lesser degree. Among the observatories the best fit is observed at KAK and KNZ observatories and the largest discrepancy is detected at KNY and MMB observatories. To investigate how the day-to-day variability in the Sq source affects the results we perform Sq

modellings for 2000 March 18 (200/194.8), which is adjacent to the spring day of 2000, already analysed. Fig. 4 presents the predicted and observed daily variations of  $Z$  for this day. One can see that the fit between 3-D predictions and observations for the less quiet day (March 18 is not Q\*-day) appears to be compatible with the fit for the neighbouring Q\*-day.

For comparison we also present year 2000 predictions and observations at Chinese observatory BMT located far inland from the deep ocean. Fig. 5 shows the variations of  $Z$  for this observatory in a similar manner as in Figs 2–4. As expected the 1-D and 3-D predictions at this site are very close to each other. Agreement with observations is also very good, with exception for Spring day however, where the fit is slightly worse.

The presented results, resolving in the principle causative mechanism of the anomalous variations in Japan, demonstrate, however, the following fact: for the major part of the data (it is especially true for summer days) the observations and predictions disagree in many details, in particular in peak-to-peak magnitudes. This is most probably due to the cumulative effect of complicated conductance distribution in this region and some inaccuracy in the ionospheric (inducing) currents as provided by the CM4 model. Indeed, the CM4 model is an approximation of the actual characteristics of the ionospheric currents with an assumption of a 1-D electrical conductivity model of the Earth. As a consequence, ocean induction effects are ignored in the CM4 model. Since this model is based not only on observatory data but also on satellite data, this assumption affects the determination of the ionospheric currents, as satellites pass over both continents and oceans. Moreover CM4 is not originally designed to describe the day-to-day variability of ionosphere currents, since monthly means of  $F_{10.7}$  have been used when deriving the model.

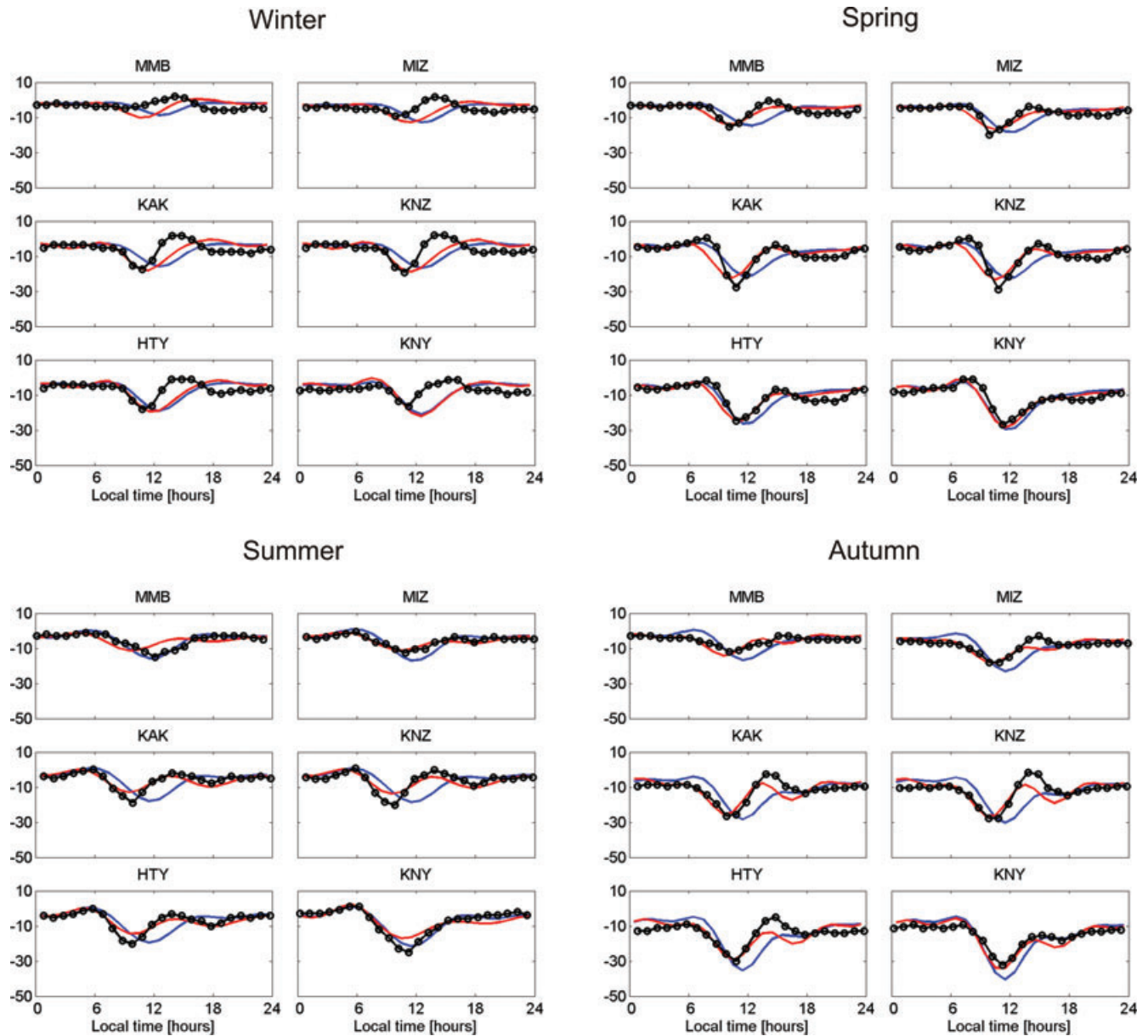


**Figure 2.** Predicted and observed daily variations of  $Z$  as a function of local time for six Japanese observatories and for four days from different seasons of 1997. Black with circles, blue and red lines are observations, 1-D (without oceans) and 3-D (with oceans) predictions, respectively.

### 3.2 Effect from changes in the near-surface conductance map

Although inaccuracy in the inducing ionospheric current system is believed to be the main reason for disagreement between the observations and predictions we should not exclude the possibility that some of discrepancy is due to ignoring the effects from deeper (mantle) 3-D heterogeneities in our model studies. In the next subsection we will examine this question. Another potential source of the discrepancy may be an inaccuracy in the near-surface conductance map. Indeed the conductance map is derived heuristically and not based on any geomagnetic data. To examine to what extent the changes in the near-surface conductance map affect the predicted  $Z$  variations we perform calculations with a suit of models in which we vary the parameters of the conductance map. As was

mentioned in Section 2, the conductance map in work (coded as the C1 map hereinafter) is based on bathymetry, salinity, temperature and pressure in oceanic regions and on sediment thicknesses in both oceanic and continental regions. In addition, we construct six alternative conductance maps (coded as C2, C3, etc. maps) that approximate real conductance distribution in a (slightly) different manner. The C2 map is based on bathymetry and sediment thickness, thus ignoring variations of salinity, temperature and pressure in the oceans. Mean conductivity of sea water,  $\sigma_w$  (which is used to calculate conductance in the oceanic regions as a product of conductivity and ocean's depth) is taken as  $3.2 \text{ S m}^{-1}$ . In C3–C7 maps the conductance in the oceanic regions is based on bathymetry only, whereas inland the conductance,  $S_c$ , is assigned to be constant. These maps differ by the adopted sea water conductivity and inland value of conductance. More explicitly, in C3, C4 and C5 maps,  $\sigma_w$



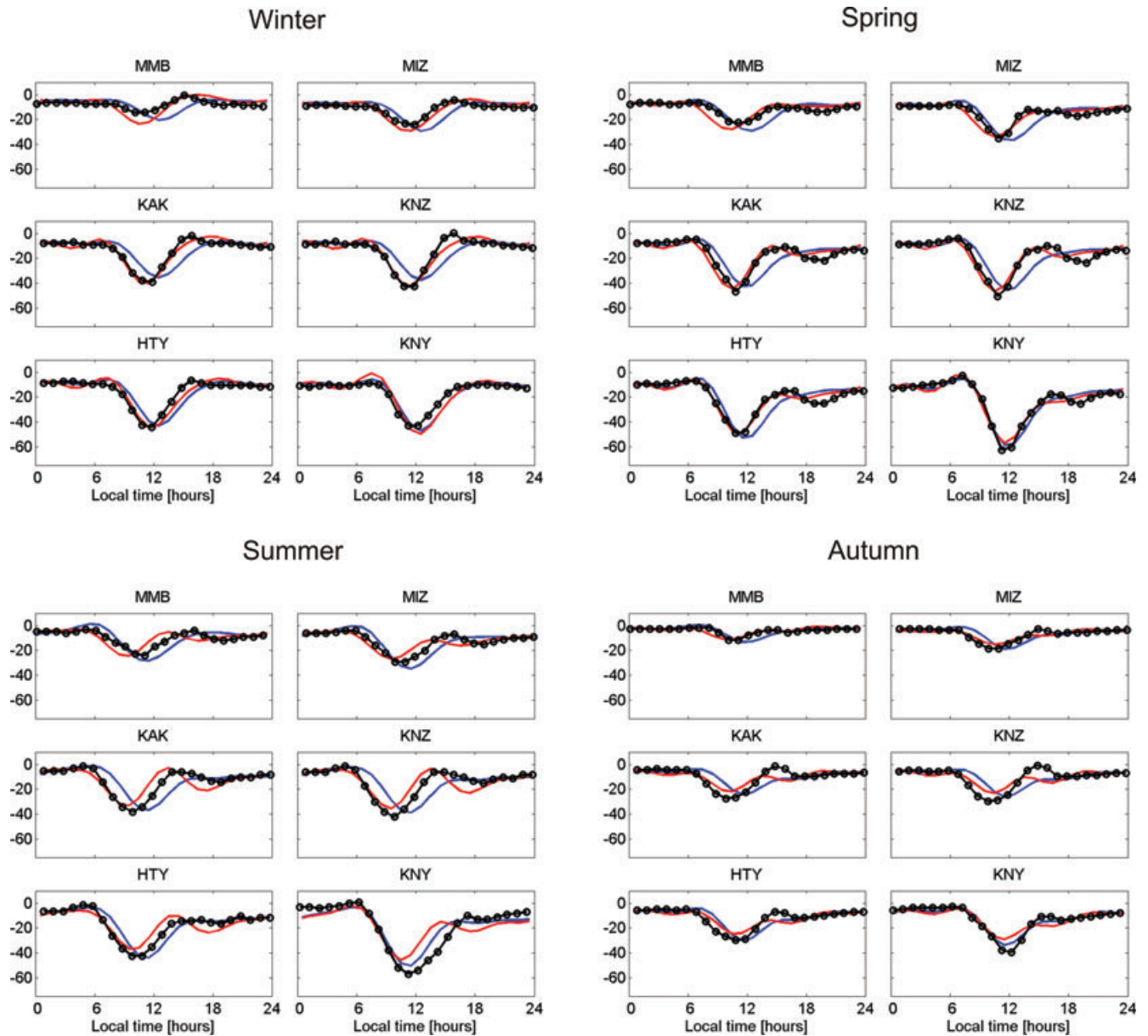


**Figure 3.** Predicted and observed daily variations of  $Z$  for four days from different seasons of 2000 year. Same legend as in Fig. 2.

is fixed to be  $3.2 \text{ S m}^{-1}$ , whereas  $S_c$  is taken as 4 S, 40 S and 400 S, respectively. In the C6 and C7 maps we fix  $S_c$  as 40 S and  $\sigma_w$  is taken as  $3.0 \text{ S m}^{-1}$  and  $3.5 \text{ S m}^{-1}$ . Fig. 6 demonstrates the results of these model studies. Note that in these and further model studies we present the results for 2000 March 17, when we see good (but not perfect) agreement between observations and 3-D predictions. Our hope was that by varying the conductance map or incorporating into the model the deeper 3-D structures we can improve the overall fit of the predictions and the data. It is seen from the plots in Fig. 6 that affordable changes in the near-surface conductance affect the results to a small extent. (Note that similar model studies performed by Shimizu *et al.* (2010) for the longer period geomagnetic responses of magnetospheric origin are in accord with this conclusion.) Due to the aforementioned possible inconsistency in the source we refrain from discussing whether predictions with one or another alternative conductance map reproduce the observations better than with the C1 map.

### 3.3 Effect from 3-D anomalies in the mantle

In this subsection, we estimate effects from subducting slab and mantle wedge, the next (after ocean) essentially 3-D and potentially important structures in the region. Note that Rikitake (1956) proposed a model with a depression of mantle conductor to account for the anomalous behaviour of the geomagnetic field variations in Japan, surprisingly before the discovery of plate subduction. First we examine whether the presence of resistive slab is required by observations. We assume that the slab has a width of 200 km and extends in a north–south direction along the coast from the ocean side. The slab in the model starts from the northern part of Honshu and has a length of 1500 km (the projection of the slab’s roof onto the Earth’s surface is shown by the dashed white line in Fig. 1). With respect to the depth, the slab extends with a dipping angle of  $45^\circ$  from the depth of 100 km to depth of 410 km where it stretches

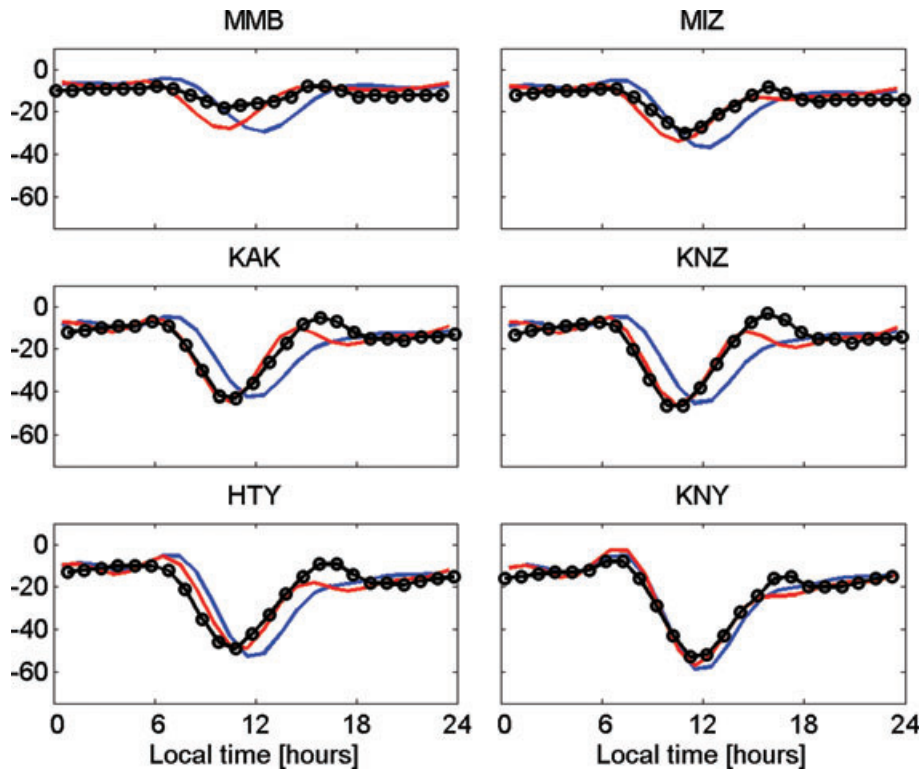


**Figure 4.** Predicted and observed daily variations of  $Z$  for 2000 March 18. Same legend as in Fig. 2.

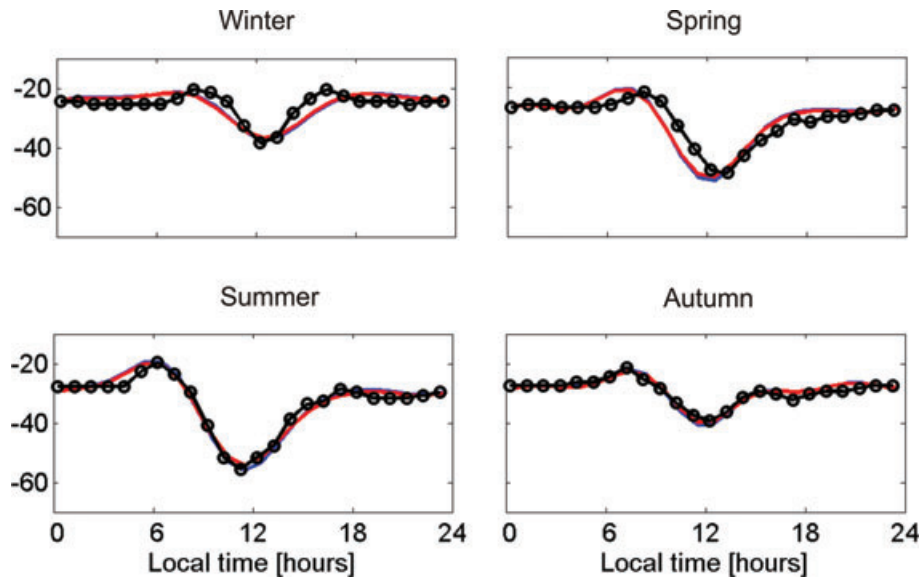


**Figure 5.** Predicted and observed daily variations of  $Z$  for Chinese observatory Beijing Ming Tombs (BMT) for four days from different seasons of 2000. Same legend as in Fig. 2.

parallel to layering 2000 km westward. We put conductivities of slab versus depth as one fifth of the host conductivities (side view of the model is shown in Fig. 7). Red dashed lines in Fig. 8 show the predictions from this model. One can see that the inclusion of 3-D resistive slab into the model produces almost invisible changes in the results.

Now we further complicate the model. Recent 3-D inversion findings by Koyama *et al.* (2006) and Kelbert *et al.* (2009) suggest a hydrated (and thus more conducting) transition zone beneath Japan. To mimic this situation, we modify the model by addressing the

conductivity of the subducting slab in the transition zone five times higher in value than the host conductivity. The location of the region with the enhanced conductivity is depicted in Fig. 7 by the dashed red line. Predictions for this model are shown in Fig. 8 as the magenta curves. It is seen that the effect from the hydrated transition zone is visible but, again, small compared with the ocean effect.

The last model we consider consists of the resistive slab already discussed and the conducting mantle wedge to the west of the slab. The location of the wedge is shown in Fig. 7 by the dashed green line. We put the conductivity of the wedge five times higher than

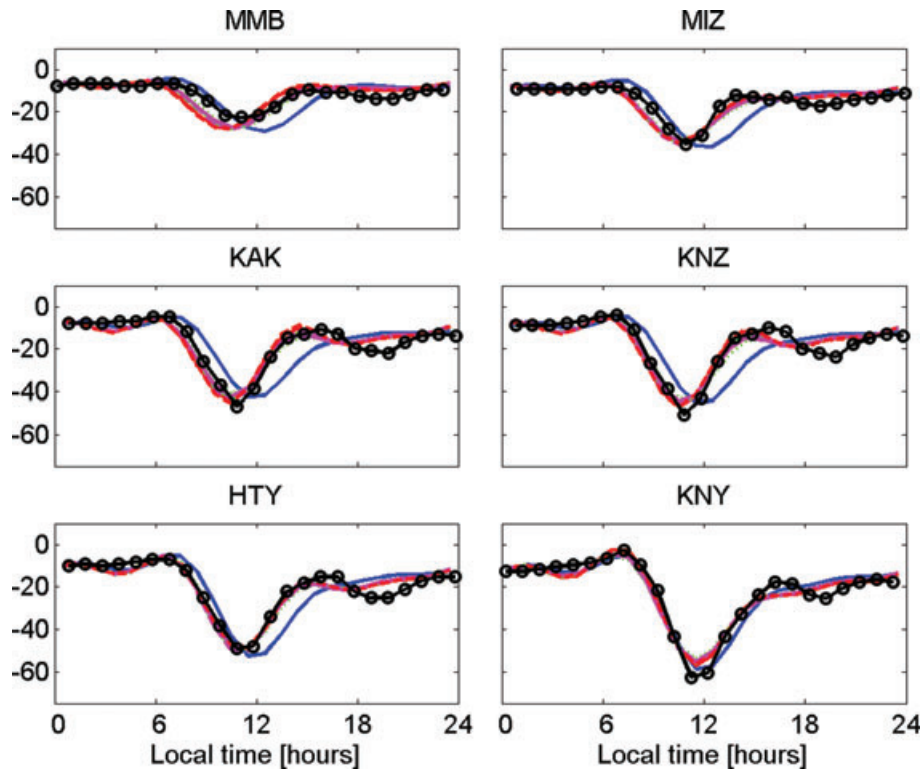


**Figure 6.** Predicted and observed daily variations of  $Z$  for 2000 March 17. Black lines with circles are observations, blue lines – predictions from 1-D model (without oceans), other lines – predictions from 3-D models with the ocean (approximated by different conductance maps) and 1-D section underneath. Red, dashed red, green, dotted green, magenta, dashed magenta are 3-D predictions with respective C1, C2, ..., C7 conductance maps. See deciphering of C1–C7 maps in the text.

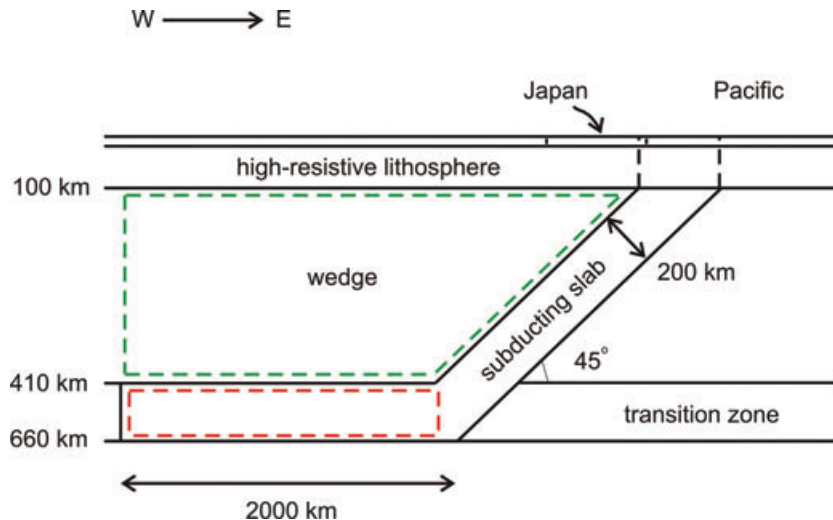


**Figure 7.** Side view of 3-D models with subducting slab (with and without enhanced conductivity in transition zone) and mantle wedge. Location of wedge is shown by dashed green line. The location of the region with the enhanced conductivity in transition zone is depicted by dashed red line. Vertical dashed lines project the roof of the slab on the Earth's surface. See plane view of this projection in Fig. 1.

the host conductivity. Green lines in Fig. 8 present the predictions for this model. The effect from the wedge seems to be the largest amongst all considered (including effects due to the changes in the conductance map) but still is not comparable with the ocean effect. As in the case with the model studies with different conductance maps we avoid the discussion of whether these, more complicated 3-D models, reproduce the observations better than the initial 3-D model with non-uniform oceans and 1-D mantle underneath. We leave this question open until we will be able to construct more

accurate inducing current systems. Hopefully with the improved source, rigorous (either regional or global) 3-D inversion of  $S_q$  data will be possible.

Finally, we investigate to what extent the  $S_q$  variations in horizontal components are affected by the oceans. Fig. 9 presents the predicted and observed daily variations of  $X$  (northward component; two left columns) and  $Y$  (eastward component; two right columns) for Japanese observatories at 2000 March 17. As expected the 1-D and 3-D predictions in both components are very close and follow

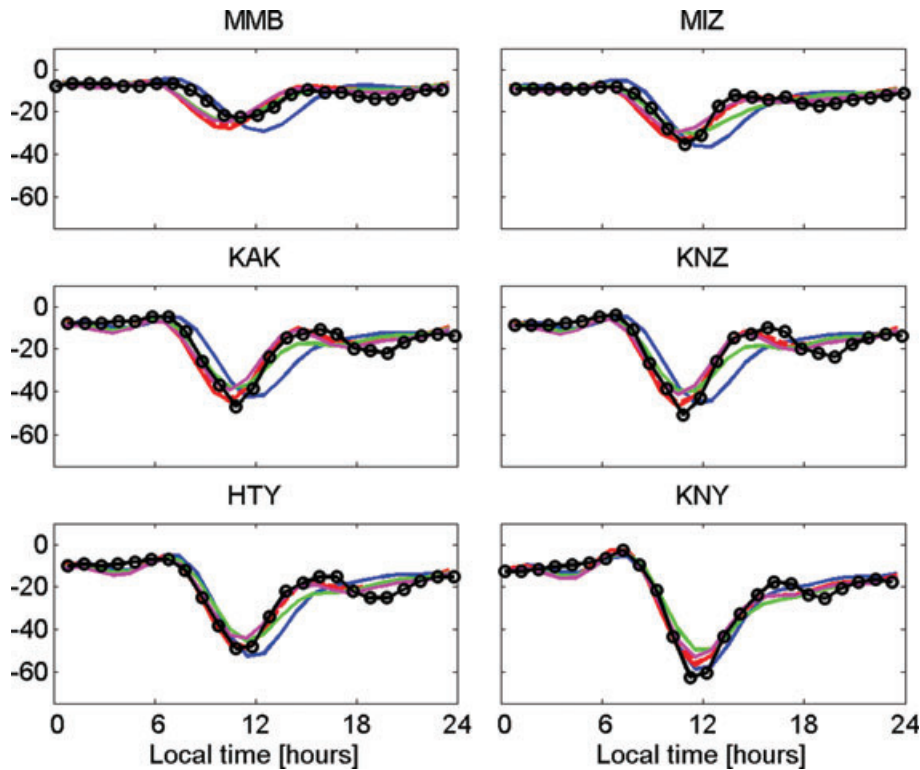


**Figure 8.** Predicted and observed daily variations of  $Z$  for 2000 March 17. Black lines with circles are observations, blue lines – predictions from 1-D model (without oceans), red solid lines – predictions from 3-D model with the ocean and 1-D section underneath. Red dashed lines – predictions from 3-D model with the ocean and subducting slab, green lines – those from 3-D model with the ocean, subducting slab and mantle wedge, magenta lines – those from 3-D model with the ocean and subducting slab, where slab is more conducting in transition zone. See details in the text.

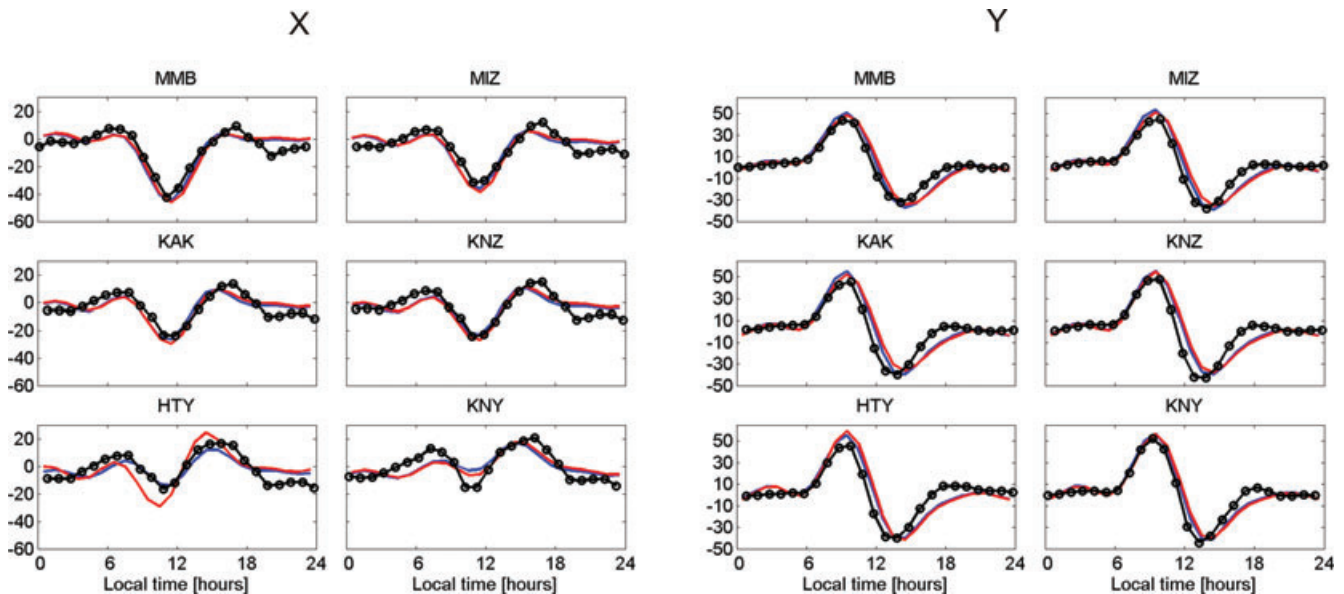


**Figure 9.** Predicted and observed daily variations of  $X$  (northward component; two left columns) and  $Y$  (eastward component; two right columns) for six Japanese observatories for 2000 March 17. Same legend as in Fig. 2.

the observations, except  $X$  variations at HTY and KNY. At HTY, a significant discrepancy is notable between the 1-D and 3-D predictions of the  $X$  component. This can be interpreted as the effect of the excess induced current flowing in the E–W direction in the ocean above which the station is located. Such an effect may not be expected for the other polarization (with the electric current flowing

in the N–S direction), which behaves as quasi TM mode due to the presence of the southern coast of Japan. Therefore there is rather a good agreement between the 1-D and 3-D predictions of the  $Y$  component at HTY. On the other hand, we note a significant discrepancy between the predictions and the observation at KNY, although the 1-D and 3-D predictions look almost identical. This discrepancy



can be ascribed (again) to the inaccuracy in the Sq source field model.

#### 4 CONCLUSIONS

We have clearly showed that anomalous behaviour of the vertical component  $Z$  of the geomagnetic Sq daily variation field at observatories in central and northern Japan – namely about a two-hour shift of the local noontime peak towards morning hours – is predominantly due to the ocean (coast) effect. This result also implies that there is no need to assume electrical conductivity anomaly in the mantle beneath central Japan, as previously suggested to explain major features of the observed anomalous behaviour in daily variations of  $Z$ .

To confirm this conclusion, we examined how the changes in the near-surface conductance map affect the computed  $Z$  variations and found that such changes influence the predictions to rather a small extent. We also demonstrated that the effects from deeper 3-D structures, such as electrically resistive subducting slab or/and the conducting mantle wedge or/and the hydrated transition zone, are also essentially weaker compared with the effect from the ocean.

However, resolving in principle the causative mechanism of the anomalous variations we see that for the major part of the considered data the observations and predictions disagree in details. Not disclaiming the possibility that some part of this disagreement comes from ignoring some unknown 3-D effects, we believe that most of the disparity is attributed to an inaccuracy in the ionospheric (inducing) currents as provided by the CM4 model. A possible way to improve the accuracy in the ionospheric source description would be a spherical harmonic analysis of global ground-based data just for the days in work (as it was done, for example, by Schmucker 1999), along with regression analysis (cf. Kleinbaum *et al.* 1987) to detect statistically significant spherical harmonics describing the source. With the improved Sq source, rigorous 3-D inversion of ground-based Sq data for constraining 3-D conductivity distribution in the upper mantle either on global or regional scale is a natural next step we plan to consider.

#### ACKNOWLEDGMENTS

This study was conducted during visiting fellowship of Alexei Kuvshinov in the Earthquake Research Institute, with a partial support by the Stagnant Slab Project (Grant-in-Aid for Scientific Research on Priority Areas #16075204). Authors express their gratitude to the staff of the geomagnetic observatories who has been collecting and distributing the data. The editor (Mark Everett) and two anonymous reviewers are acknowledged for their helpful comments.

#### REFERENCES

- Campbell, W., 1989. The regular geomagnetic field variations during quiet solar conditions, in *Geomagnetism*, Vol. 3, ed. Jacobs, J.A., Elsevier, New York, pp. 385–460.
- Everett, M.E., 2006. Local time stacking of geomagnetic solar daily variations, *J. geophys. Res.*, **111**, B03103, doi:10.1029/2005JB003831.
- Everett, M.E., Constable, S. & Constable, C.G., 2003. Effects of near-surface conductance on global satellite induction responses, *Geophys. J. Int.*, **153**, 277–286.
- Kelbert, A., Schultz, A. & Egbert, G., 2009. Global electromagnetic induction constraints on transition-zone water content variations, *Nature*, **460**, 1003–1007.
- Kleinbaum, D.G., Kupper, L.L. & Muller, K.E., 1987. *Applied Regression Analysis and other Multivariable Methods*, p. 718, PWS-KENT Publishing Company, Boston.
- Koyama, T., Shimizu, H., Utada, H., Ichiki, M., Ohtani, E. & Hae, R., 2006. Water content in the mantle transition zone beneath the North Pacific derived from the electrical conductivity anomaly, *Am. geophys. Monogr. Ser.*, **168**, 171–179.
- Kuvshinov, A., 2008. 3-D global induction in the oceans and solid Earth: recent progress in modeling magnetic and electric fields from sources of magnetospheric, ionospheric and oceanic origin, *Surv. Geophys.*, **29**, 139–186.
- Kuvshinov, A., Avdeev, D. & Pankratov, O., 1999. Global induction by Sq and Dst sources in the presence of oceans: bimodal solutions for non-uniform spherical surface shells above radially-symmetric earth models in comparison to observations, *Geophys. J. Int.*, **137**, 630–650.
- Kuvshinov, A., Manoj, C., Olsen, N. & Sabaka, T., 2007. On induction effects of geomagnetic daily variations from equatorial electrojet and solar quiet sources at low and middle latitudes, *J. geophys. Res.*, **112**(B10102), 13, doi:10.1029/2007JB004955.
- Laske, G. & Masters, G., 1997. A global digital map of sediment thickness, *EOS, Trans. Am. geophys. Un.*, **78**, F483.
- Manoj, C., Kuvshinov, A.V., Maus, S. & Lühr, H., 2006. Ocean circulation generated magnetic signals, *Earth, Planets and Space*, **58**, 429–437.
- Rikitake, T., 1956. Electrical state and seismicity beneath Japan, *Bull. Earthq. Res. Inst., Univ. Tokyo*, **34**, 291–299.
- Rikitake, T., Yokoyama, T. & Sato, S., 1956. Anomaly of the geomagnetic Sq variation in Japan and its relation to the subterranean structure, *Bull. Earthq. Res. Inst., Univ. Tokyo*, **34**, 197–234.
- Sabaka, T.J., Olsen, N. & Purucker, M., 2004. Extending comprehensive models of the Earth's magnetic field with Oersted and CHAMP data, *Geophys. J. Int.*, **159**, 521–547.
- Schmucker, U., 1999. A spherical harmonic analysis of solar daily variations in the years 1964–65. I. Methods, *Geophys. J. Int.*, **136**, 439–454.
- Shimizu, H., Koyama, T., Baba, K. & Utada, H., 2010. Revised 1-D mantle electrical conductivity structure beneath the north Pacific, *Geophys. J. Int.*, **180**, 1030–1048.
- Takeda, M., 1993. Geomagnetic field variation on the ground by the electric currents in the oceans induced by the geomagnetic Sq field, *J. Geomag. Geoelectr.*, **45**, 487–493.